



Studying ZnO:Al's Structural and Optical Characteristics by Chemical Spray Pyrolysis Method

Sundus M.Meteab*, J.F. Mohammad

Department of Physics, Faculty of Education for Pure Science, University of Anbar, Anbar, Iraq

*Corresponding Author: e-mail: sun21u3003@uoanbar.edu.iq

Keywords:

Thin Films;
Doping;
XRD;
Optical Properties;
Zno:Al;
Spray Pyrolysis.

Abstract

In this study, pure zinc oxide films doped with (Al) were prepared by spray pyrolysis technique, with percentages of (3,5 and 7%) and molar concentrations (0.05), on glass substrates at a temperature of (350 °C). X-ray diffraction pattern showed that pure zinc oxide films are all polycrystalline and have a hexagonal structure with a preferred growth direction (002). Using atomic force microscopy (AFM), the surface topography of the produced films was investigated. The findings that emerged from the analysis demonstrated a reduction in the membrane's surface roughness after doping as well as a reduction in particle size (126-55.64nm). Besides, the scanning electron microscopy (FE-SEM) results of all generated films were examined and reviewed in order to understand the composition of their surfaces and to determine the particle size, in order that practically all surfaces are covered with the spherical particles, which are collected longitudinally into ribbon-like structures linked to one another. On the other hand, optical properties have shown that the values of the energy gap for direct transitions increased from (3.73 eV) for pure films to (3.80 eV) for aluminum doped films. The optical properties investigation included transmittance spectrum, absorption coefficient and energy gap. The transmittance (89%) was within the visible spectrum region.

Introduction

Today, one of the best ways to learn about the physical and chemical characteristics of materials that are difficult to get in their native form is to examine deposited materials in the form of thin films. Because it deals with tiny devices and is now a separate part of solid-state physics, thin-film physics is one of the more recent fields whose significance has grown. One of the key technologies that advanced the research of semiconductors, particularly transparent conducting oxides (TCO) like zinc oxide (ZnO), is thin film technology [2]. Zinc oxide, as depicted in figure 1, is a transparent conductive oxide that is significant due to its unique qualities, including high optical transparency within the visible range and good chemical and mechanical stability. With an energy gap of roughly 3.3 eV and a low cost in comparison to other materials, zinc oxide is an n-type semiconductor material. Since the second half of the seventeenth century, researchers

have been working on the preparation of thin films. As a result of their introduction into a variety of industries for the production of interference filters, detectors, and other thin electronic device components have a wide range of applications today. Considering their diminutive size and low weight, they have started building electronic digital accounts and creating space research gadgets [2]. Numerous studies have been conducted on doping for (ZnO), one of the materials available and easily to precipitate, with several elements, including (Al, Cu, Au, Ag, Mg) [4]. ZnO is one of the easily-precipitated materials available. The addition of some metal ions as impurities significantly and significantly contributes to changing the concentration of charge carriers and causing changes in the crystalline structure and others at the level of electrical conductivity. An element with the symbol Al and atomic number (13), aluminum is a metal that belongs to the boron group of elements. Bauxite ore is the principal source of aluminum. Aluminum's small weight and resistance to corrosion makes it unique, as it is employed in the aviation sector. Corrosion resistance in aluminum is particularly strong [5]. It is preferable to use transparent conductive oxides in the majority of applications because they have good electrical and optical properties, an energy gap that is equal to or greater than (3 eV), good conductivity in the range of ($10^3 \Omega \cdot \text{cm}$), and a high transparency of up to (80%) in the visible field [6].

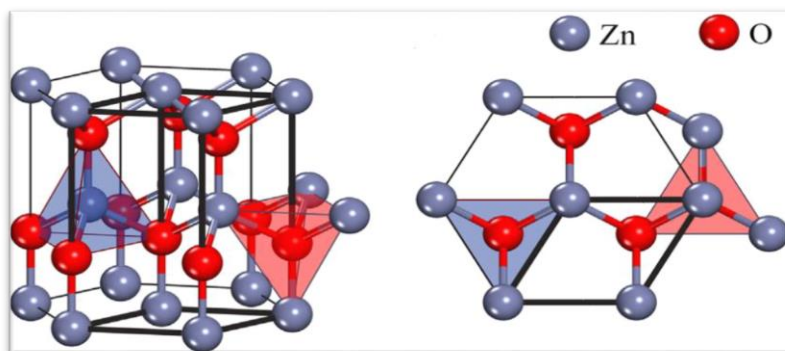


Figure 1. Crystal structure of zinc oxide [7].

Experimental procedure

Zinc chlorides with a purity of 97% and a molecular weight of (M_w -136.31g), made by the Indian company Himedia, have been Utilized. The solution was made with a weight of $W = 0.136 \text{ g}$, a molar concentration of 0.05 M, and was dissolved in 100 ml of distilled water. At a temperature of 50 °C, the produced solution is blending for 30 minutes using a magnetic stirrer. In order to assure the homogeneity of the solution and to ensure that there are no contaminants in it, we obtained the solution and let it sit for an hour before starting the spraying procedure. Obtaining metal oxide coatings is done by spraying a $\text{ZnCl}_2 \cdot 2\text{H}_2\text{O}$ solution at a temperature of 350 °C. The films made in various ratios under ideal conditions underwent structural, optical, and electrical tests. Aluminum chloride was used to dope (ZnO) with aluminum (Al), which is (3%, 5%, 7%), and it was prepared at a molar concentration of (0.05 M) and dissolved in (100 ml) of distilled water. The aluminum chloride was then added in different volume percentages (3%, 5%, 7%) to the zinc chloride

solution, where it was first deposited on the glass. Obtaining the required weight is achieved through deposition by using the following equation [8]:

$$M = \left(\frac{W_t}{M_{wt}} \right) \cdot \left(\frac{1000}{V} \right) \dots \dots \dots (1)$$

Where: M is the molar concentration, W_t : is the weight that needs to dissolve, and M_{wt} : is the substance's molecular weight, V: the amount of distilled water used to create the solution.

Results and discussion:

XRD Results:

Since X-ray diffraction is an effective method for determining the effects of the treatment of the crystallization of materials, it has been investigated to understand the nature of the crystal structure of various materials. For instance, a recent study [9] employed XRD to comprehend how various treatments affected the crystallization of the sample material. Figure (2) depicts the X-ray diffraction (XRD) pattern of pure ZnO thin films doped with aluminum (Al) at a doping percentage of (3%, 5%, 7%), prepared by chemical spray pyrolysis method at a concentration of (0.05) molar and at a temperature of (350 °C), and then deposited on glass bases with a range ($2\theta = 20-80^\circ$). The examination's findings demonstrated that the produced films had a polycrystalline and hexagonal structure with crystal growth along several crystal orientations (100), (002), (101), (102), (103), (004). As can be seen from the figure, there are eight peaks that correspond to the diffraction angles (32.76°), (34.09°), (36.32°), (47.60°), (62.94°) and (72.71°), respectively, where all peaks match well with Bragg reflections of the hexagonal structure as per the standard numbered (No.36-1451.JCPDS card) [10,11]. The distinctive and favored direction was (002). Thus, there is no phase due to aluminum or its compounds [12]. The crystal size of the prepared pure and doped films was calculated for the dominant direction (002) at the angle (34.09°) using the (Debye-Scherrer) equation [13]:

$$D_{ave} = \frac{k\lambda}{\beta \cos \theta} \dots \dots \dots (2)$$

β is the "FWHM" (Full-Width-Half-Maximum) curve's middle width measured in radial units of radian, θ ; the Bragg angle, λ ; the wavelength of the incoming rays; and k: a shape factor of 0.94. We see that the crystal size decreases from (21.23) nm to (15.71) nm, and that the intensity decreases with an increase in the half-width of the beam at the dominating peak (FWHM), as shown in table (1). These outcomes are in line with the researchers' findings [14].

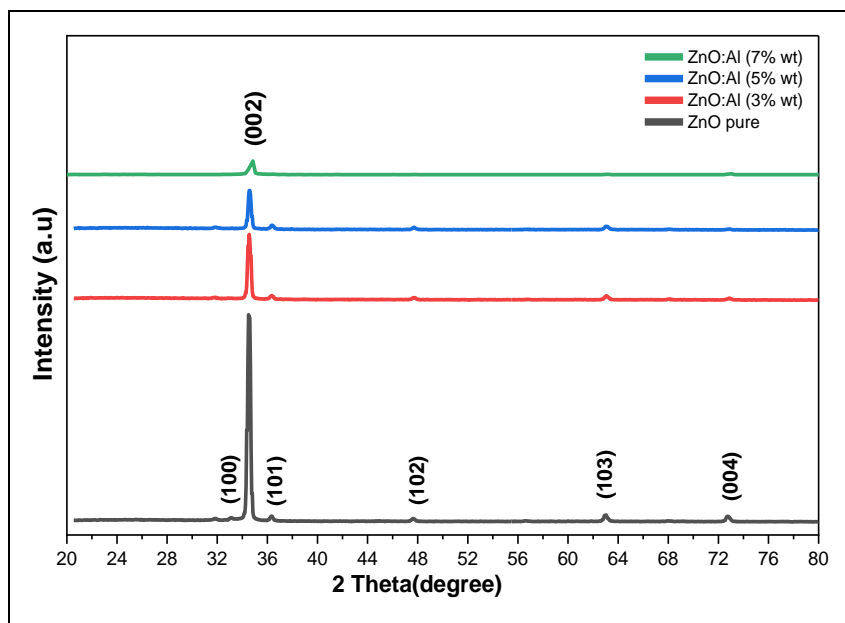


Figure 2. X-ray diffraction of pure ZnO film doped with aluminum in different proportions (3%, 5%, 7%).

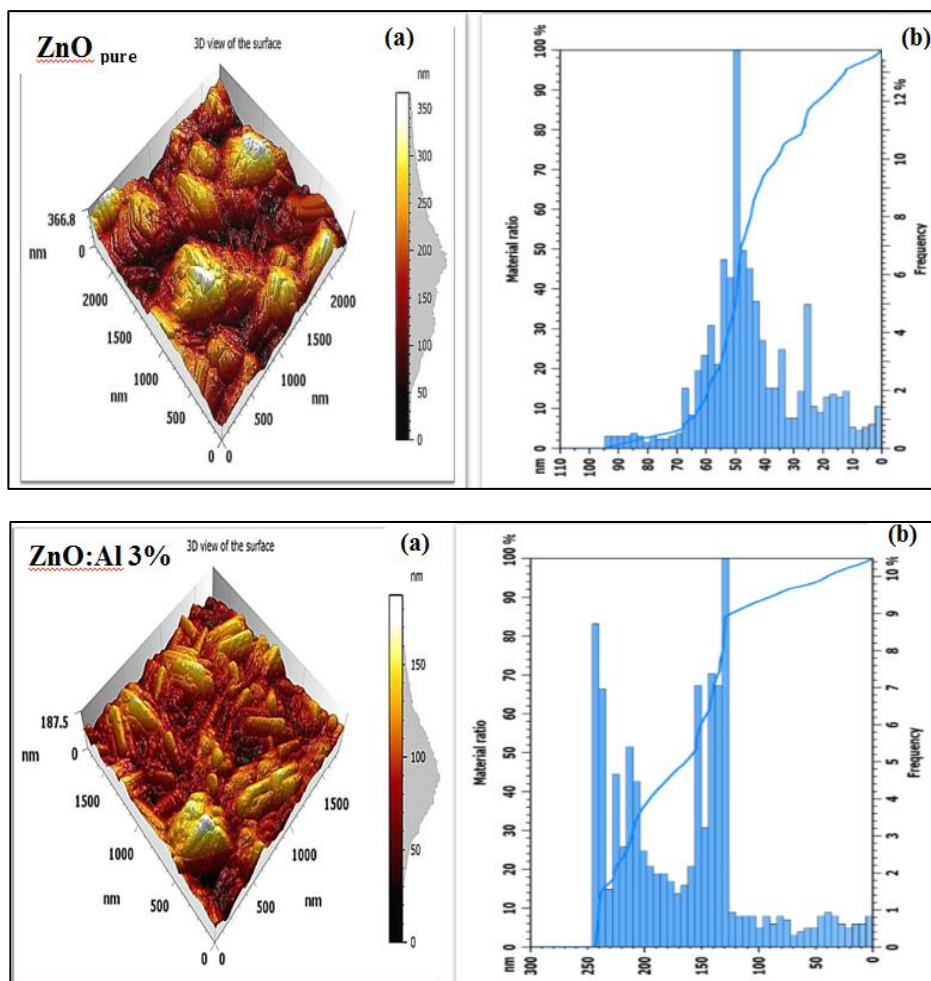
Table 1. shows the X-ray diffraction results of pure ZnO films doped with aluminum.

Samples	2Theta (deg)	d(hkl) Å	(hkl)	Crystalline size(D)nm
ZnO Pure	34.09	2.627	(002)	21.23
ZnO:Al 3%	34.51	2.596	(002)	19.22
ZnO:Al 5%	34.52	2.595	(002)	17.65
ZnO:Al 7%	34.55	2.593	(002)	15.71

AFM Results:

Studying the created film's surface characteristics and parameters is one of the matters that should be done because of its characteristics; a significant impact on the manufacturing devices' effectiveness. Accordingly, the topography of the pure zinc oxide surfaces was examined using an atomic force microscope (AFM), which has a great capacity for providing precise statistical values for the grain size rate. Figure (3) depicts pure and inlaid zinc oxide films created by the chemical method of spray pyrolysis and deposited on glass bases in three dimensions, as well as volume distribution photographs. (Avg. Diameter), measuring 126.0 nm, and the film's average surface roughness, measuring 63.82 nm, and the film's mean square root value was (79.17 nm), either in the case of Al-doping or in varied proportions (3%, 5%, 7%). The average surface roughness of thin film was (63.82 nm), and with an increase in doping rate, we see that the average particle size gradually lowers and

that the membrane's surface roughness also reduces. The smallness of these figures suggests that as doping increases, the size of the particles decreases. As a result, the film has more surface area, which increases the number of processes that take place there. These characteristics of the inserted thin film surfaces allow us to employ them for a variety of applications, including photovoltaics. We note that there is an agreement between the results of AFM and XRD regarding the size decrease. This is because the granular size measured by AFM is greater than the crystal size measured by XRD, since the XRD measures the size of the crystals inside the film, and the AFM measures the size of the granules at the surface which is larger than the inside and is consistent with what the researchers discovered [15,16].



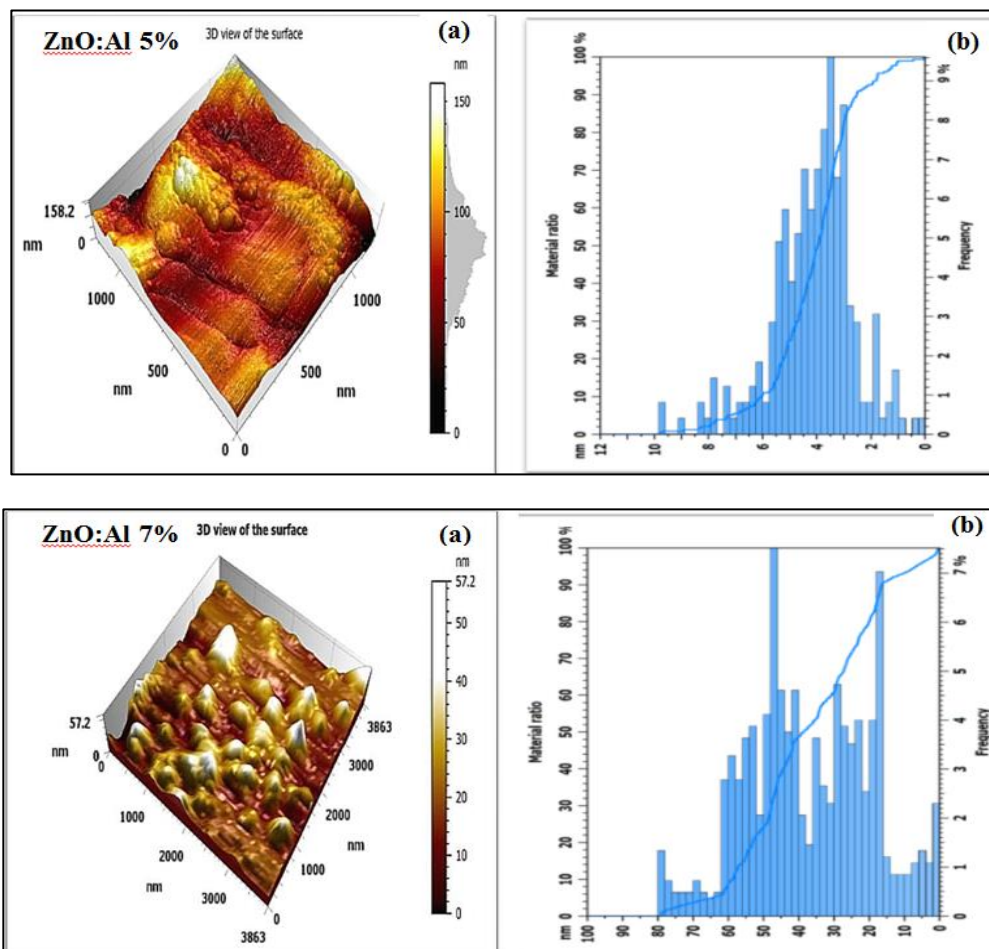


Figure 3. AFM images of pure zinc oxide doped with aluminium (ZnO:Al) in different ratios (3%, 5%, 7%): (a) a picture in three dimensions, (b) the particle size distribution.

Table 2. Atomic force microscopy results of pure (ZnO) films doped with aluminum.

Sample	Root mean square (nm)	Roughness average (nm)	Average grain size (nm)
ZnO	79.17	63.82	126.0
ZnO: Al 3%	59.78	48.01	106.1
ZnO: Al 5%	23.97	18.97	92.44
ZnO: Al 7%	19.73	15.22	55.64

FE-SEM Results:

All of the prepared films' scanning electron microscope (FE-SEM) data were examined and analyzed in order to learn more about the surface characteristics of the prepared films and to establish the particle size. Figure (4) displays pictures taken with a scanning electron microscope at a magnification of (100.0 X) and a

resolution of up to 200 nm for pure zinc oxide films that have been thermally decomposed and deposited on glass bases and then doped with aluminum at a doping ratio of (3%, 5%, or 7%). When comparing the images, it is observed that the pure films that were created (part - a -) are distinguished by being free from minute flaws like pinholes or cracks, and that practically all surfaces are covered with the spherical particles, which are collected longitudinally into ribbon-like structures linked to one another.

The average particle size of the membrane components is (55.97 nm), and this behavior is consistent with the findings of researchers [17]. It is noted that the inoculation rates (3%, 5%, and 7%) part (b, c, and d) of the figure and the films inlaid with aluminum were also homogeneous, i.e., there was no chance of the so-called thin film peeling process, which is brought on by the difference in thermal expansion coefficients during the thermal treatment for the spread of the occurring impurities.

This indicates the quality of the prepared films and the efficiency of the system used in the process of sedimentation, as well as the good adhesion characteristic of the prepared films with the glass bases. It is noted that an abundant layer of small Nano-granules of semi-spherical shape is distributed homogeneously and with great regularity over the surface area of the sample to form a larger agglomeration of the aluminum-grafted membranes that tend to form flower-like structure.

As it is clearly shown, the nano-granules after the impurity process helped to change the surface morphology [18], it was found that the average particle size at the ratio (3%) is (55.26) nm and the ratio (5%) is (27.13) nm, while the ratio (7%) is (27.09) nm, a decrease in the particle size with the increase in doping with aluminum At (3%), (5%), and (7%); this is consistent with the results of XRD.

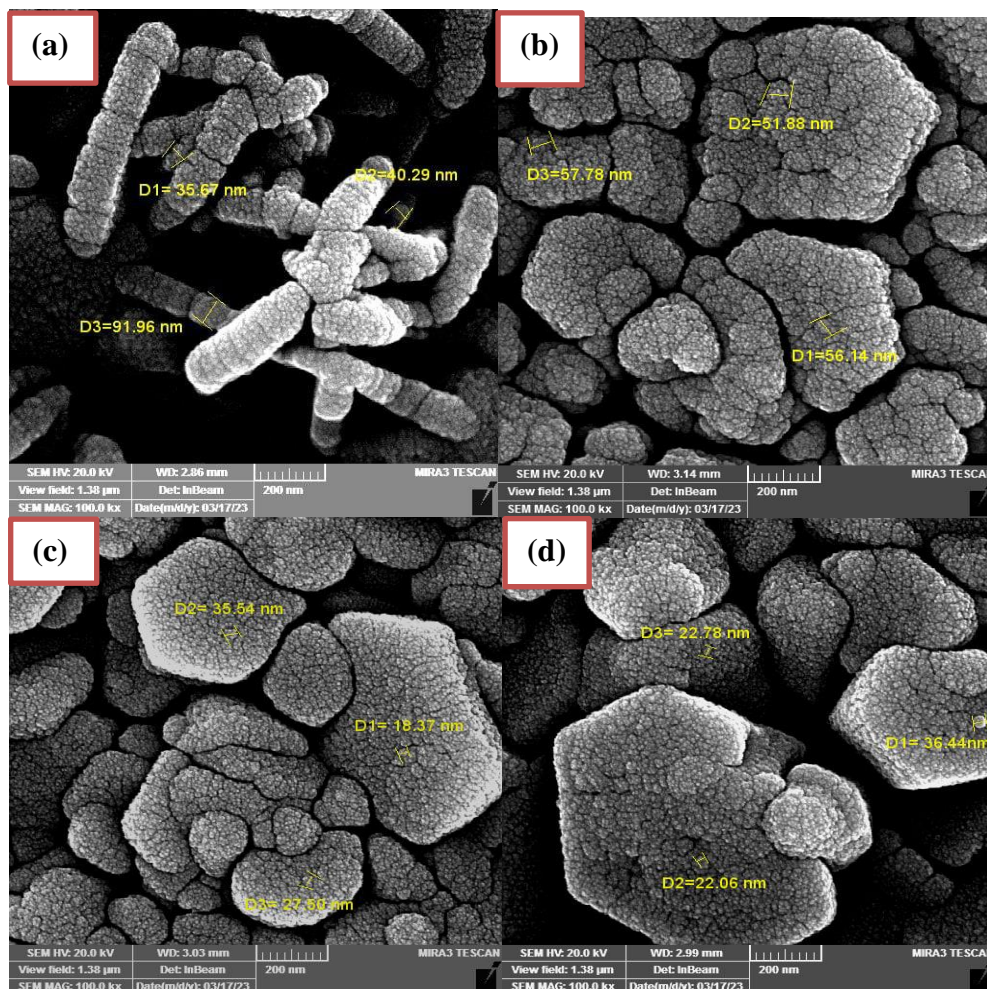


Figure 4. FE-SEM images of ZnO films: (a) pure, (b) doped with aluminum (3% Al), (c) doped with (5% Al), (d) doped with (7% Al).

Optical Properties Analysis

Transmittance Spectrum:

The transmittance spectrum measurements were made for all prepared films, both pure and doped, within the wavelength range (300-1100) nm. The behavior of the transmittance spectrum for all the prepared samples is the greatest at the long wavelengths of the few photon energies, and then it increases as it approaches the short wavelengths, as shown in figure (5), which compares the change of the transmittance spectrum as a function of wavelength for the pure and doped aluminum zinc oxide films with doping rates of (3%, 5%, 7%) respectively. The permeability of the pure film reached up to (78%). The figure illustrates how the additional impurity increased the permeability of the manufactured films in the instance of the inserted films. We observe that following the doping with aluminum (Al) in amounts (3%, 5%, 7%), the permeability started to rise. As demonstrated in table (3) at the same length, the transmittance increased from (78%) in the wavelength (550 nm) to roughly (89%) when impurifying by (7%). And this is due to the density of region formed by the atoms of the doped material in the original material between the valence and conduction bands, the less scattering

effect and structural homogeneity is the reason for the increased transmittance of the films, which is consistent with the researcher in (Y.Larbah, et.al.) [19].

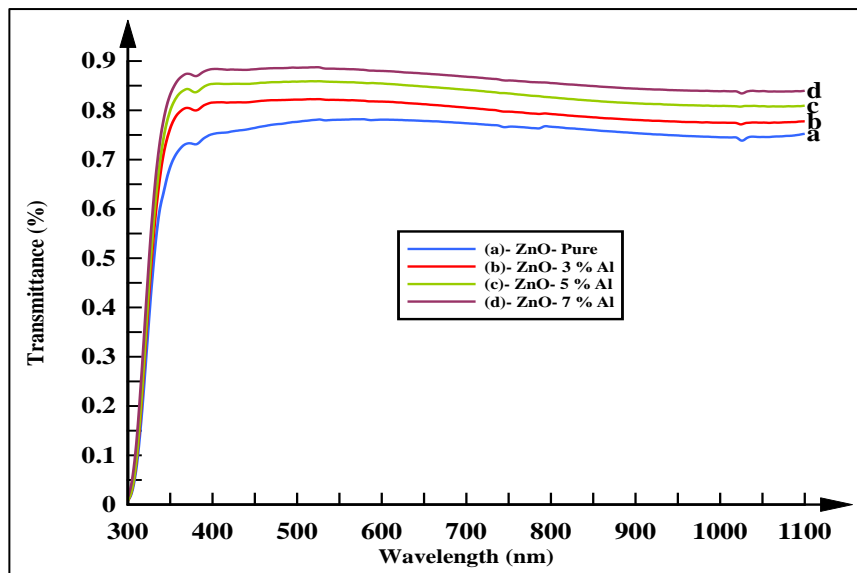


Figure 5. Transmittance as a function of wavelength for pure (ZnO) films doped with aluminum.

Table 3. The permeability values of the pure ZnO film doped with aluminium, at rates of (3%, 5%, and 7%) at a temperature of (350 °C) and a molar concentration of (0.05 M).

Samples	Transmittance (%) at (550 nm)
ZnO-Pure	78%
ZnO: 3% Al	82%
ZnO: 5% Al	86%
ZnO: 7% Al	89%

Absorption Coefficient:

The absorption coefficient of pure zinc oxide films doped with aluminum was calculated. Figure (6) shows the change of the absorption coefficient as a function of the wavelength of the pure zinc oxide films dotted with aluminum and with doping rates of (3%, 5%, 7%). Due to their proportionality, absorption (α) and the behavior of the absorption spectrum are quite similar. It can be inferred that the band gap is direct based on the values of the absorption coefficient ($\alpha > 10^4\text{cm}^{-1}$) in the system. We observe that the absorption coefficient drops as the proportion of aluminum doping is increased. This might be due to the incident photon's energy which is less than the semiconductor's optical energy gap, making it impossible for it to excite the electrons and move them from the valence band to the conduction band. It also becomes clear to us that the absorption

coefficient decreases with the increase in the percentage of copper doping due to the low absorbency of the prepared films. This is due to the fact that the incident photons at high wavelength do not have enough energy to interact with the atoms, so the incident photon will be transmitted. This is in line with earlier research [19-21].

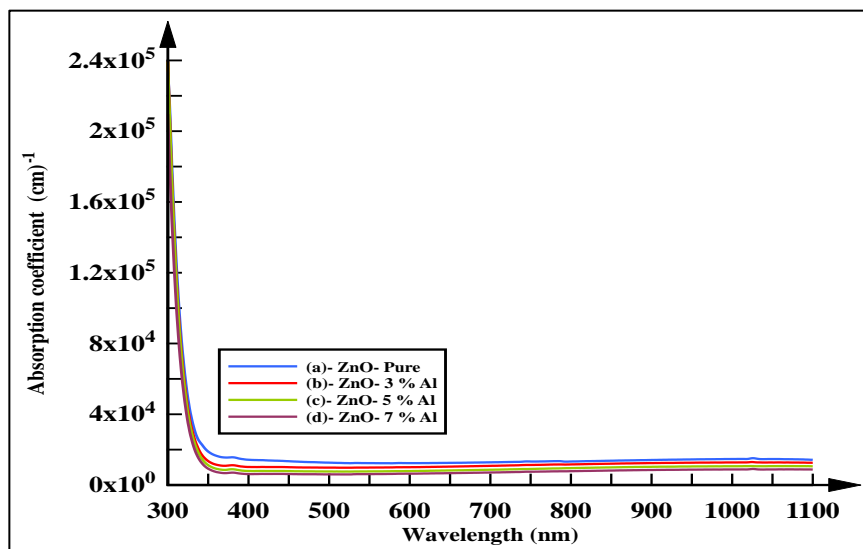


Figure 6. Absorption coefficient as a function of wavelength of pure (ZnO) film doped with aluminium, prepared at a temperature (350 °C) and a molar concentration (0.05 M).

Energy Gap:

The value of the energy gap for the direct allowed transitions was calculated through the (Tauc) model by drawing the relationship graphically between the projected photon energy ($h\nu$), and from the extension of the straight part of the resulting curve to intersect with the photon energy axis at the point ($\alpha h\nu^2 = 0$), then we get the value of the optical energy gap for the direct transmission allowed and for all the films prepared, through figure (7). It was found that the energy gap value of the ZnO film is equal to (3.73 eV), and this value corresponds to what was published previously [22], and that the energy gap for the same membrane after doping it with aluminum (Al) increased by (3%) to (3.76 eV). After grafting by (5%) it increased to (3.77 eV) until the energy gap for (7%) reached (3.80 eV) as shown in table (4). This means that the grafting has led to the displacement of the absorption edge towards higher energies, and this increase can be explained as a result of the so-called Burshstain-Moss shift. Energy increases [23,24].

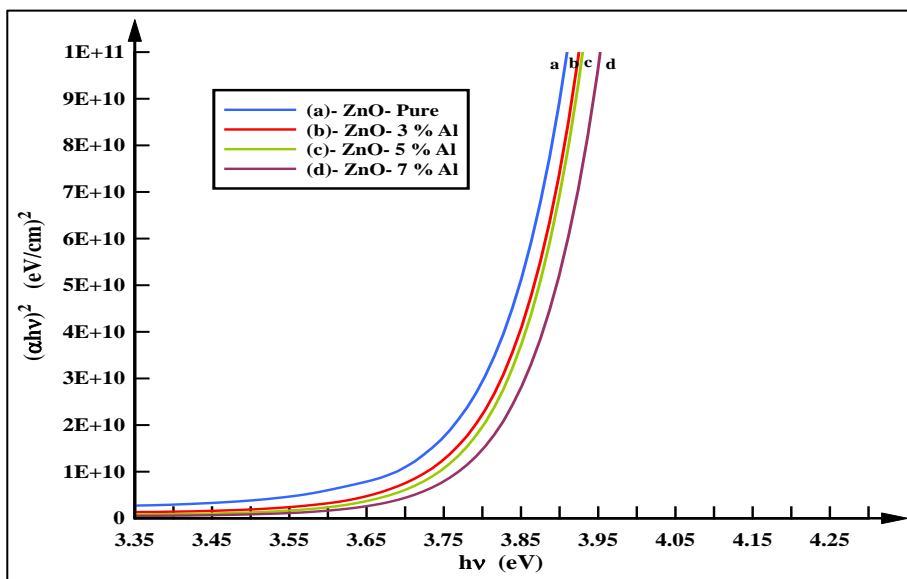


Figure 7. The optical energy gap of pure ZnO film doped with aluminum in different proportions.

Table 4. shows the energy gap value of pure ZnO film doped with aluminium.

Samples	Optical Energy Gap (eV)
ZnO-Pure	3.73
ZnO: 3% Al	3.76
ZnO: 5% Al	3.77
ZnO: 7% Al	3.80

Conclusion:

The ZnO:Al thin films were deposited on glass bases using chemical a spray pyrolysis method (CSP) at a temperature of (350 °C) and with different percentages of aluminum doping. The results of (XRD) showed that the ZnO films have a polycrystalline hexagonal structure with a preferred orientation (002) and that the crystal size decreases when doped with aluminum from (21.23 nm) to (15.71 nm). The AFM results also showed a decrease in the particle size and surface roughness (RMS) of the (ZnO) samples doped with (Al). Microscopic images of FE-SEM examination show that the particles are spherical in shape, grouped longitudinally in the form of bands linked to each other and distributed almost over all parts of the film, and the average particle size is (55.97) nm. The results of the optical properties showed that the greatest value of transmittance is (89%) for the grafted films within the visible or near-infrared range of the wavelength region. Also, there was a decrease in the absorption coefficient of zinc oxide films when doped with aluminum, and the direct energy gap ranged between (3.73-3.80 eV). Thus, ZnO:Al exhibits excellent structural and optical properties, which makes it suitable for use in photovoltaic applications.

References

- [1] S. A. Hussein, and G. J. Abdel-Sada, "The effect of copper casting on the optical properties of the ZnFe₂O₄ Zinc membranes", *Kerbala Scientific University Journal*, vol. 16, Issue 1, pp. 131-126,(2018).
- [2] A. N. Saleh, A. I. Hassan, "Study the effect of the type and nature of the substrate on the optical properties of the thin films of (NiO) prepared by spin coating method", *Tikrit Journal of Pure Sciences*, No. 20, No. 1,20, pp. 131-126,(2018).
- [3] J.Farden, *Hand book of modern sensors*,(2003).
- [4] L. Eckertova , "Physics of Thin Films, Plenum presses, New York and London (1977).
- [5] Aluminum Association. *Aluminum: properties and physical metallurgy*. ASM international. (1984).
- [6] L. Castañeda, *Review of Conducting Oxides Semiconductors in Thin Solid Films*. *Biomedical Journal of Scientific & Technical Research*, 41(1), 32261-32270. (2022).
- [7] W. Liu, S.Wang, J.Wang, B.Zhang, L.Liu, H. Liu, & J. Yang, *Supercritical hydrothermal synthesis of nano-zinc oxide: Process and mechanism*. *Ceramics International*, 48(16), 22629-22646. (2022).
- [8] G. Busch, H. Schade, "Lectures on Solid State Physics", Pergamon Press, London, (1976).
- [9] J. K. Sjöström, R. Bindler, T. Granberg, & M. E. Kylander., *Procedure for organic matter removal from peat samples for XRD mineral analysis*. *Wetlands*, 39, 473-481, (2019).
- [10] Khalid Haneen Abass , Musaab Khudhur Mohammed "Fabrication of ZnO:Al/Si Solar Cell and Enhancement its Efficiency Via Al-Doping" *Nano Biomed. Eng.*, , Vol. 11, Iss. 2 doi: 10.5101/nbe.v11i2.p170-177. (2019).
- [11] N.Ahmed, M. S.Hassan, & M.Hassan, *Effects of aluminum (Al) incorporation on structural, optical and thermal properties of ZnO nanoparticles*. *Materials Science-Poland*, 36(3), 419-426, (2018).
- [12] M.Maache , Devers, T., & Chala, A. *Al-doped and pure ZnO thin films elaborated by sol-gel spin coating process for optoelectronic applications*. *Semiconductors*, 51, 1604-1610, (2017).
- [13] G. L.Tan, D.Tang, D.Dastan, A.Jafari, J. P.Silva, & X. T. Yin, *(Effect of heat treatment on electrical and surface properties of tungsten oxide thin films grown by HFCVD technique*. *Materials Science in Semiconductor Processing*, 122, 105506, (2021).
- [14] K. N.Tonny, R.Rafique, A.Sharmin, , M. S. Bashar, & Mahmood, Z. H. *Electrical, optical and structural properties of transparent conducting Al doped ZnO (AZO) deposited by sol-gel spin coating*. *AIP Advances*, 8(6), 065307. (2018).
- [15] M. Shirazi, R.S. Dariani, M. R. & Toroghinejad, *Influence of doping behavior of Al on nanostructure, morphology and optoelectronic properties of Al Doped ZnO thin film grown on FTO substrate*. *Journal of Materials Science: Materials in Electronics*, 27, 10226-10236. (2016).
- [16] N.Srinatha, P.Raghu, H. M.Mahesh, &B. Angadi, *Spin-coated Al-doped ZnO thin films for optical applications: Structural, micro-structural, optical and luminescence studies*. *Journal of Alloys and Compounds*, 722, 888-895 . (2017)
- [17] V.Saxena, P. Chandra, & L. M. Pandey, *Design and characterization of novel Al-doped ZnO nanoassembly as an effective nanoantibiotic*. *Applied Nanoscience*, 8, 1925-1941, (2018).
- [18] S. U. OffiahS. N. Agbo & P. Sutta & M. Maaza & P. E. Ugwuoke & R. U. Osuji & F. I. Ezema "Study of the extrinsic properties of ZnO:Al grown by SILAR technique", *J Solid State Electrochem* -DOI 10.1007/s10008-017-3514-6,(2017).
- [19] Y.Larbah, M.Adnane, & B.Rahal, *Growth and characterization of ZnO and Al-doped ZnO thin films by a homemade spray pyrolysis*. *Semiconductors*, 54, 1439-1444.(2020) .
- [20] S.Hossain, , G. D. A. Quaderi, , K. M. A.Hussain, , & T. Faruqe, *Synthesis and Characterization of Undoped and Aluminum Doped Zinc Oxide Thin Films using Thermal Evaporation Method*. *Nuclear Science and Applications*, 27(1&2).(2018) .
- [21] A.Riaz, A.Ashraf, H.Taimoor, S.Javed, M. A.Akram, M.Islam, ... & Saeed, K. *Photocatalytic and photostability behavior of Ag-and/or Al-Doped ZnO films in methylene blue and rhodamine B under UV-C irradiation*. *Coatings*, 9(3), 202.(2019) .
- [22] L.Dejam, S.Kulesza, J.Sabbaghzadeh, A.Ghaderi, S.Solaymani, Ş. Ṫalu, & A.hossein Sari, *ZnO, Cu-doped ZnO, Al-doped ZnO and Cu-Al doped ZnO thin films: Advanced micro-morphology, crystalline structures and optical properties*. *Results in Physics*, 44, 106209.(2023) .

- [23] P.Raghu, N.Srinatha, C. S.Naveen, H. M.Mahesh, & B.Angadi, Investigation on the effect of Al concentration on the structural, optical and electrical properties of spin coated Al: ZnO thin films. *Journal of Alloys and Compounds*, 694, 68-75.(2017) .
- [24] D.Ali, M. Z.Butt, I.Muneer, F.Bashir, M.Hanif, T. M.Khan, & S. A. Abbasi Synthesis, characterization and antibacterial performance of transparent c-axis oriented Al doped ZnO thin films. *Surfaces and Interfaces*, 27, 10145.(2021) .